Title

Retro-orbital and disseminated B-cell lymphoma in a yellow-collared macaw (Primolius auricollis).

Journal

Canadian Veterinary Journal, 58(7)

ISSN

0008-5286

Authors

Le, Kim
Beaufrère, Hugues
Brouwer, Emily
et al.

Publication Date

2017-07-01

Peer reviewed

Case Report Rapport de cas

Retro-orbital and disseminated B-cell lymphoma in a yellow-collared macaw *(Primolius auricollis)*

Kim Le, Hugues Beaufrère, Emily Brouwer, S. Karlyn Bland, Sarah Wills, Shawn MacKenzie, Heather Chalmers, Chantale Pinard, R. Darren Wood, Josepha DeLay, Dale A. Smith

Abstract — A yellow-collared macaw was presented with unilateral left exophthalmia. The complete blood cell count and biochemistry revealed a heterophilic leukocytosis and elevation in liver parameters, respectively. A computed tomography scan showed a contrast-enhancing retrobulbar mass and hepatomegaly. Cytology of the liver was consistent with a round cell tumor, most likely lymphoma. The bird died after 2 months of palliative care. Postmortem examination confirmed a retro-orbital and disseminated B-cell lymphoma.

Résumé — Lymphome B rétro-orbital et disséminé chez un ara à collier jaune *(Primolius auricollis).* Un ara à collier jaune a été présenté avec de l'exophtalmie unilatérale gauche. La formule sanguine complète et la biochimie ont révélé une leucocytose hétérophile et une élévation des paramètres hépatiques, respectivement. La tomodensitométrie à l'aide d'une injection de milieu de contraste a montré une masse rétrobulbaire et une hépatomégalie. La cytologie du foie était conforme à une tumeur à cellules rondes, le plus probablement un lymphome. L'oiseau est mort après 2 mois de soins palliatifs. L'examen postmortem a confirmé un lymphome B rétro-orbital et disséminé.

(Traduit par Isabelle Vallières)

Can Vet J 2017;58:707–712

Case description

A 20-year-old female yellow-collared macaw *(Primolius auricollis)* was presented to the Ontario Veterinary College Health Sciences Centre for an acute onset of left ocular swelling. The owners reported that the bird had a decreased appetite for 3 days prior to presentation. There was no sneezing, discharge, or irritation in the head region noted by the owners. The bird had no prior relevant medical history. The macaw was fed a complete pelleted diet, supplemented with fruits and vegetables.

On physical examination, the bird weighed 223 g and had a body condition score of 3/5. There was evidence of feather damaging behavior throughout the plumage. There was left exophthalmia and associated peri-ocular swelling. Dazzle and palpebral reflexes were present and the fundic examination was unremarkable. No abnormalities were detected in the right eye. Oropharyngeal examination revealed a small white plaque deep within the choanal slit dorsal to the boney roof of the *fossa choanalis,* and the bird's beak was found to be unexpectedly brittle when held open with a speculum. Hepatomegaly was suspected on coelomic palpation and visual examination. A blood sample was taken from the right jugular vein and placed into EDTA and heparin tubes, which were submitted for a complete blood (cell) count (CBC) and plasma biochemistry analysis, respectively.

Hematology revealed a moderate heterophilic leukocytosis [WBC 35.1 $\times$ 10^9/L, heterophils 28.4 $\times$ 10^9/L; reference interval (RI) for *Ara* spp., no reference intervals available for *P. auricollis:* WBC: 7 to 22 $\times$ 10^9/L] (1), and evidence of a left shift (band heterophils 3.86 $\times$ 10^9/L). A mild anemia (41%; RI: 47 to 55%) (1) with evidence of mild polychromasia [(5 to 10 per high power field (HPF)] was present. These findings were interpreted as indicative of inflammation and mild regenerative anemia. Plasma biochemistry showed mild hypoproteinemia (30 g/L; RI: 34 to 42 g/L) (1). Also present were marked elevations in activity of aspartate aminotransferase (AST; 1936 U/L; RI: 124 to 378 U/L) (1), creatine kinase (3202 U/L; RI: 35 to 355 U/L) (1), glutamate dehydrogenase (GLDH; 27 U/L; RI:

Health Sciences Centre (Le, Beaufrère, Wills), Department of Clinical Studies (MacKenzie, Chalmers, Pinard), Department of Pathobiology (Brouwer, Bland, Wood, Smith), Ontario Veterinary College; Animal Health Laboratory (DeLay), University of Guelph, Guelph, Ontario N1G 2W1.

Dr. Le's current address is Sydney Exotics and Rabbit Vets, North Shore Veterinary Specialist Hospital, 64 Atchison St, Crows Nest NSW 2064, Sydney, Australia.

Dr. Wills' current address is Exotic Animal Care Centre, Pasadena, California, USA.

Dr. MacKenzie's current address is Toronto Veterinary Emergency Hospital, 21 Rolark Drive, Scarborough, Ontario M1R 3B1.

Address all correspondence to Dr. Hugues Beaufrère; e-mail: beaufrer@uoguelph.ca

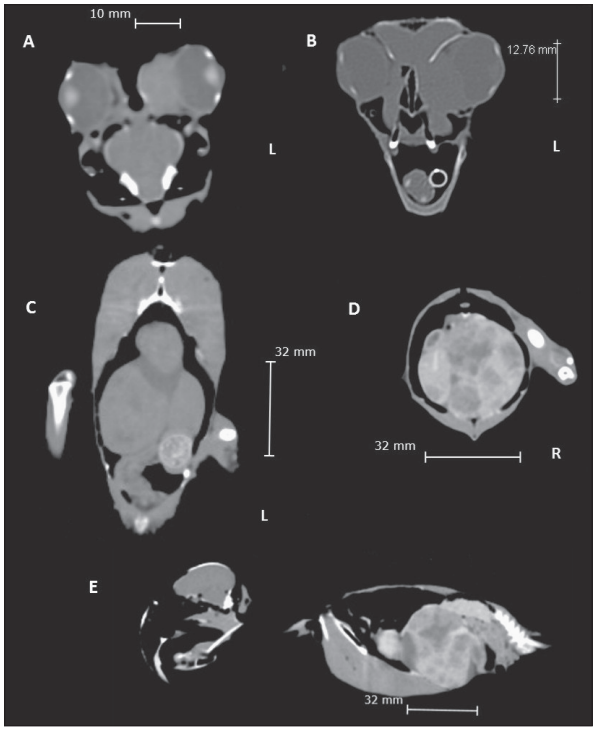

Figure 1. Contrast CT-scan images of the head and body of a yellow-collared macaw *(Primolius auricollis)* with multi-organ B-cell lymphoma. Coronal (A) and transverse (B) sections of the head with a retrobulbar mass visible medial to the eye on the right side of the image (left side of the bird). Coronal (C), transverse (D), and sagittal (E) sections of the body illustrating hepatomegaly and multifocal, rounded, irregularly marginated hypoattenuating nodules with mild, non-uniform contrast enhancement. Scale bars depict size and boundaries of hepatic outline.

< 8 U/L) (1), and a mild elevation in bile acids (85 μmol/L; RI: < 71 μmol/L) (1). The GLDH elevation was consistent with hepatic necrosis and the mild bile acid elevation was consistent with mild liver dysfunction or post-prandial elevation. The specific source of the elevation in AST could not be determined as there was evidence of both muscle (CK) and hepatocyte (GLDH) injury.

Computed tomography (CT) examination of the whole body was performed using a 16-slice helical scanner (GE Bright Speed; General Electric Healthcare, Milwaukee, Wisconsin, USA). The bird was sedated with midazolam (Versed; Roche Labs, Basel, Switzerland), 0.5 mg/kg body weight (BW) intranasally, mask-induced with isoflurane at 5% delivered with oxygen, and intubated with a 3 mm uncuffed endotracheal tube. Anesthesia was monitored with a Doppler unit placed on the superficial ulnar artery and with a capnograph. A 26 G intravenous catheter was placed in the right medial metatarsal vein to facilitate the administration of iopamidol, a non-ionic contrast agent (Isovue-300; Bracco Diagnostics, Monroe Township, New Jersey, USA), 2 mL/kg BW, IV, for contrast CT, which was taken approximately 3 to 5 s after completion of the injection.

Findings on the CT examination included a retro-bulbar mass of uniform density that occupied the infraorbital sinus and caused distortion of the medial aspect of the left globe as well as exophthalmia (Figures 1A, 1B). Mild heterogeneous contrast

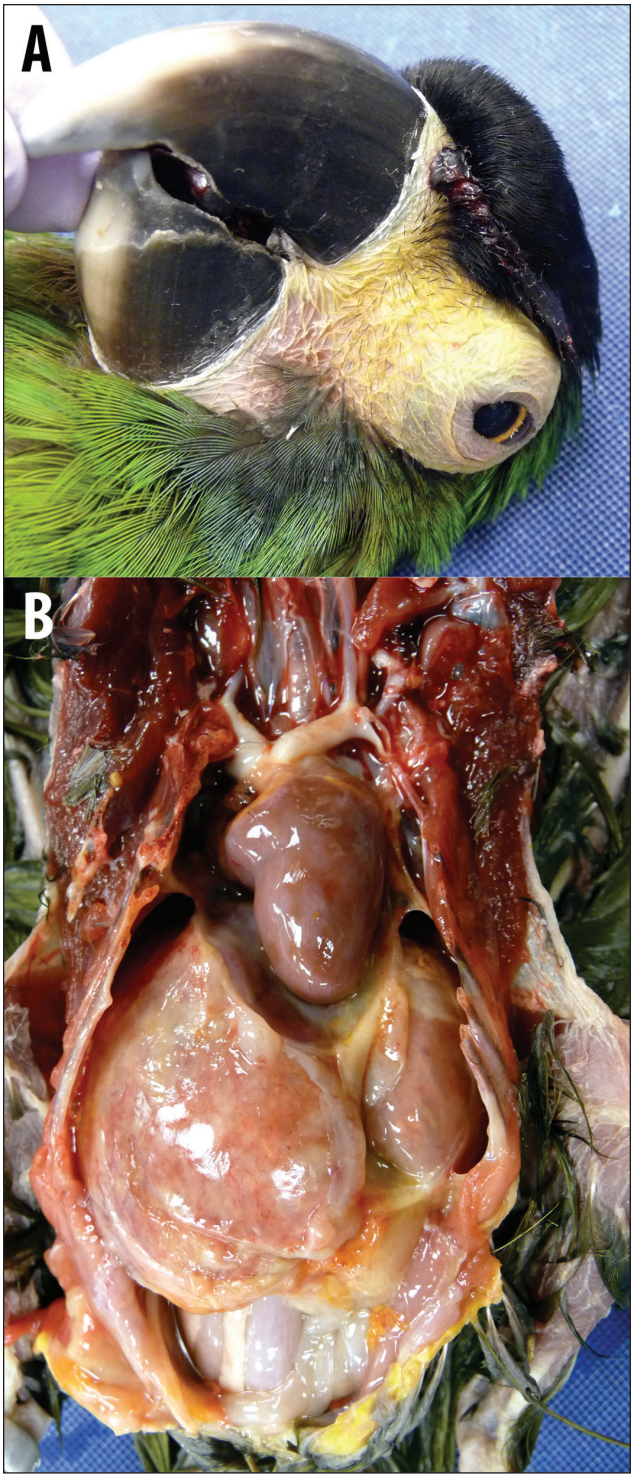

Figure 2. A – Gross necropsy image of a yellow-collared macaw *(Primolius auricollis)* with multi-organ B-cell lymphoma showing exophthalmia due to retrobulbar neoplastic infiltration. B – Gross necropsy image of a yellow-collared macaw *(Primolius auricollis)* with multi-organ B-cell lymphoma showing hepatomegaly with rounded hepatic borders, mottling, and pallor of the hepatic surface, and irregular thickening of the hepatic capsule and adjacent mesentery. Compare to Figure 1.

enhancement of the mass was noted. The liver was markedly enlarged with multifocal, rounded, irregularly marginated hypoattenuating nodules that had mild, non-uniform contrast

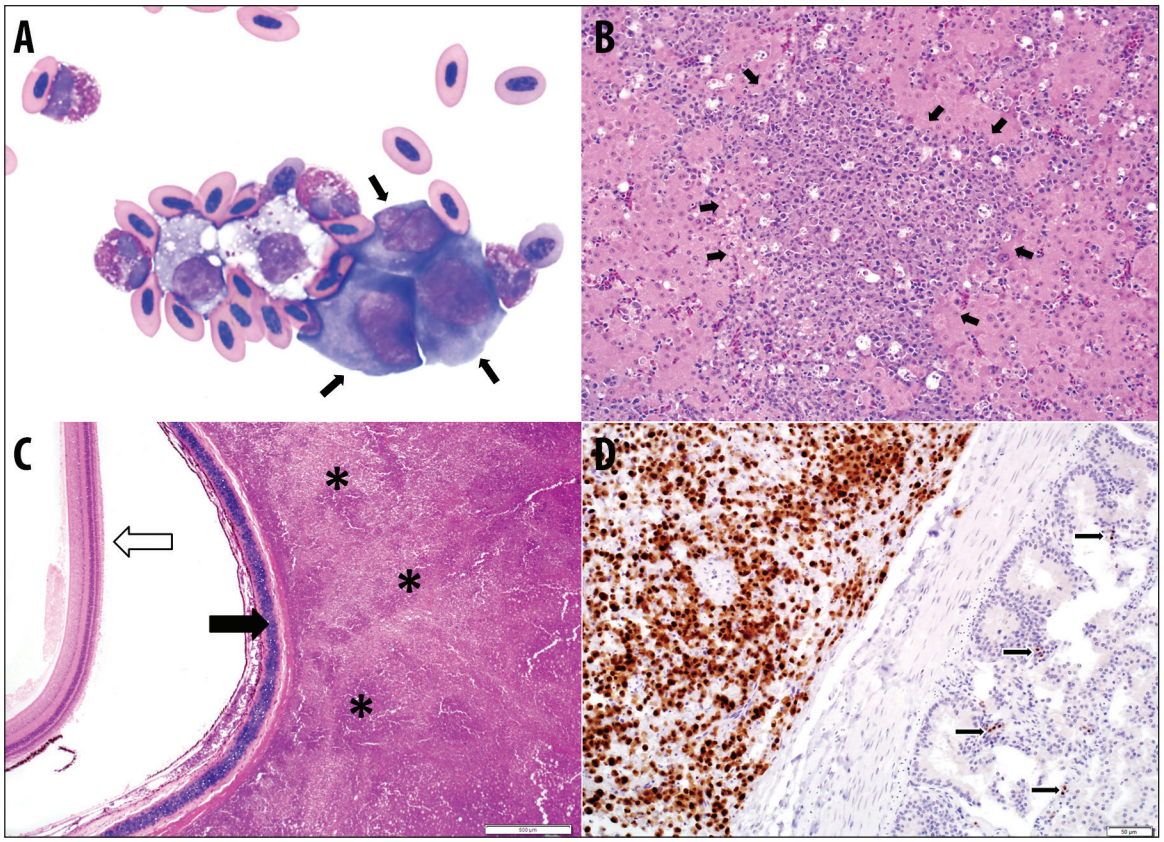

Figure 3. A – Cytologic appearance (cytospin preparation) of a fine-needle aspirate from a cystic region of a hepatic mass in a yellow-collared macaw *(Primolius auricollis)* with multi-organ B-cell lymphoma. There are neoplastic cells with deeply basophilic cytoplasm and bizarre nuclear morphology (arrows), large foamy macrophages with prominent granules, heterophils, and red blood cells. Wright's stain. Magnification 600×. B – Histologic appearance of the liver of a yellow-collared macaw *(Primolius auricollis)* with multi-organ B-cell lymphoma. There is a nodule of neoplastic cells (arrows) within the hepatic parenchyma. Hematoxylin and eosin. Magnification 200×. C – Histologic appearance of a retrobulbar mass in a yellow-collared macaw *(Primolius auricollis)* with multi-organ B-cell lymphoma. Empty arrow – detached retina (artefact); solid arrow – scleral ossicle; asterisks – neoplastic infiltrate. Hematoxylin and eosin. Bar = 500 μm. D – Immunohistochemical staining for MUM1 antigen in a section of small intestine with a serosal/mesenteric neoplastic infiltrate in a yellow-collared macaw *(Primolius auricollis)* with multi-organ B-cell lymphoma. Strong nuclear and less pronounced cytoplasmic staining are visible in a large proportion of the neoplastic cells (left side of the image), as well as in scattered cells in the lamina propria of the small intestine (arrows). Bar = 50 μm.

enhancement (Figures 1C to 1E). These nodules distorted the liver margins and displaced the ventriculus, proventriculus, and spleen caudolaterally to the left and the intestines caudally. While under anesthesia, a bradyarrhythmia with regular occasional skipped beats was identified. Two doses of glycopyrrolate (Robinul; Baxter Healthcare, Deerfield, Illinois, USA), 0.02 mg/kg BW, IV, had no effect on cardiac rate or rhythm. Anesthesia was therefore terminated prior to other diagnostic procedures being carried out.

The bird was re-anesthetized in the same manner on the following day in order to obtain fine-needle aspirates of the retrobulbar and hepatic masses. The left and right liver lobes were sampled percutaneously by direct visualization under the skin; aspiration of the right liver lobe produced 3 mL of fluid, whereas aspiration of the left liver lobe resulted in only a cellular parenchymal aspirate. The retro-bulbar mass could not be safely sampled due to the small size of the bird and the location of the mass dorsal to the palatine bone and medial to the jugal arch. The bradyarrhythmia occurred again, this time on recovery, and was again unresponsive to an anti-cholinergic agent, atropine. An electrocardiogram tracing was obtained but did not capture an appropriate sequence of bradyarrhythmia.

On cytology of the cytospin from the fluid obtained from the right liver lobe, there were numerous large individual cells with a round to angular shape exhibiting 4- to 5-fold anisocytosis, moderate anisokaryosis and with basophilic cytoplasm. Many cells were binucleate or trinucleate, and nuclei tended to be indented, bilobed, or angular with clumped chromatin. Occasionally, satellite nuclei and nuclear molding were observed. Additionally, there were frequent large vacuolated macrophages, erythrocytes, and heterophils. Occasional mitotic figures were noted. These findings were compatible with round cell neoplasia and mixed inflammation. Similar cell populations were noted on the sample from the left liver lobe, but the large cells appeared rounder, and had more deeply basophilic cytoplasm and a distinct perinuclear Golgi zone. There was moderate anisocytosis

and anisokaryosis with similar varied and atypical nuclear shapes (Figure 2A). Some cells had prominent nucleoli. These findings were similarly interpreted as round cell neoplasia.

The owner elected palliative out-patient care, declining radiotherapy for the ocular component of the disease and chemotherapeutics. The bird was initially sent home on tramadol (Novopharm, Toronto, Ontario), 10 mg/kg BW, PO, q12h; and meloxicam (Metacam, Boehringer Ingelheim Vetmedica. St. Joseph, Missouri, USA), 0.5 mg/kg BW, PO, q24h, to provide pain relief. The meloxicam was discontinued and prednisolone acetate (Rafter 8 Products, Calgary, Alberta), 0.2 mg/kg BW, PO, q24h, was administered once the cytological diagnosis was received. The bird continued to have a good quality of life, showing no clinical signs of illness, until 2 mo later when it died acutely at home. The body was submitted for necropsy.

On external postmortem examination, pronounced exophthalmos of the left globe and mild periocular swelling were noted (Figure 2A). On internal examination, the left retrobulbar region contained a 7-mm diameter soft, homogenous tan mass. There was diffuse pallor of multiple organs (liver, thyroid glands, and kidneys) and marked hepatomegaly with rounded borders and an irregular mottled pattern (Figure 2B). Approximately 6 mL of clear yellow fluid was present in the coelomic cavity along with fibrinous adhesions between the coelomic viscera and air sacs. Representative samples were fixed in 10% neutral buffered formalin, paraffin embedded, and sections stained with hematoxylin and eosin. The entire head, after removal of the brain, was placed in formalin to be sectioned after fixation and decalcification.

On microscopic examination, there was an infiltrative round cell neoplasm present within multiple organs. Infiltrating neoplastic cells had morphologic features of lymphoma, including distinct cell margins, abundant eosinophilic cytoplasm, round central to eccentric nuclei, clumped chromatin and prominent nucleoli. Many neoplastic cells had prominent perinuclear clearing, consistent with a Golgi zone. Neoplastic cells replaced approximately 90% of the hepatic parenchyma (Figure 3B) and were present in the kidney, spleen, ovary, gastrointestinal serosa, cloacal submucosa, air-sac membranes, adrenal gland, and bone marrow. Bone marrow from the tibiotarsus was 100% cellular, with erythroid and granulocytic lineages admixed with large cells resembling those described above. The distribution of the abnormal cells was patchy, encompassing 5% to 25% of the bone marrow, depending on the field of view. Of the normal resident marrow cells, the population was approximately 70% erythroid. Maturation of resident marrow cells appeared synchronous. Vascular invasion was not identified in the sections examined. The left retro-bulbar mass (Figure 3C) was composed of neoplastic cells similar to those described previously and did not appear to invade the globe or enter the cranial vault. Incidental findings included type-III atherosclerosis in the great vessels and carotid and brachial arteries (2), a schwannoma in the pectoral muscle and mild multifocal hemorrhage within the koilin layer of the ventriculus. The heart showed no histological evidence of disease.

Immunohistochemistry was performed to further identify the neoplastic cells. Strong positive nuclear and weaker cytoplasmic staining with MUM1 (monoclonal mouse anti-human MUM1 protein, clone MUM1p; Dako, Burlington, Ontario) was present in over 80% of the infiltrative cells in the liver and mesentery, as well as in scattered cells within the lamina propria of the small intestine and spleen, used as the species control tissue (Figure 3D). Additional tissue blocks from a macaw (species not provided) and a Congo African grey parrot containing bursa, spleen, and thymus were subjected to the same IHC staining protocol for MUM1 antigen and appropriate positive staining was observed in lymphoid tissue in each case. There was no CD3 (rabbit polyclonal raised against the human antigen; Dako) immunoreactivity of the neoplastic cells; however, scattered lymphocytes within the renal interstitium showed strong cytoplasmic immunoreactivity to CD3, acting as a species-specific positive control for this stain. MHC II (clone TAL.1B5, mouse monoclonal raised against the human antigen; Dako) staining was also performed, but there was no reaction with lymphocytes in the species control tissue or with the neoplastic cells. Based on the histologic and cytologic appearance of the neoplastic cells, and the positive MUM1 and negative CD3 staining, a diagnosis of B-cell lymphoma was made.

Discussion

This case describes the clinical, advanced imaging, cytological, and histological findings associated with a retrobulbar and systemic B-cell lymphoma in a yellow-collared macaw. It highlights the importance of a complete and thorough medical diagnostic work-up and how the utilization of advanced imaging and fine-needle aspiration of the liver may provide a method of obtaining a diagnosis in a non-invasive manner in an unstable patient. The infiltrative and extensive nature of the disease was defined through contrast CT. This superior imaging modality, as compared to radiography, enabled appropriate planning and staging of diagnostics in this patient.

Ultrasound is a simple and non-invasive way to obtain immediate assessment of the globe and its associated orbital structures in mammals. The anatomical re-enforcement of the avian globe by the scleral ossicles diminishes the value of ultrasound to diagnose and characterize retrobulbar diseases, though it can be useful in identifying diseases of the posterior eye segment (3). Exophthalmos is more prevalent in birds than buphthalmos and indicates a retrobulbar space occupying lesion or an extension of a malignant ocular neoplasia (4,5). Due to the complexity of the anatomy of the structures of the head, advanced imaging is more effective in delineating the topography of such lesions than are radiographs and ultrasound. While CT was the imaging modality of choice in this case, MRI could have been performed instead. While MRI has a superior soft-tissue resolution, CT was selected in this case as the scanning time is much shorter than for MRI, it does not require specific monitoring equipment that is MRI-compatible, and the MRI resolution may be low for small birds using a conventional 1.5 T MRI. An additional advantage of the rapid scanning rate of the CT is that a whole-body scan can often be performed, allowing identification of lesions in other organ systems as was seen in our case (6–8).

Lymphoma is commonly observed in avian species and typically involves the liver, spleen, and kidneys (9–11), although

infiltration of the globe and adnexal tissue (5,12–15), skin (16), and intestines (17,18) has also been identified. It is notable that many cases of retrobulbar neoplasia, including the case presented herein, are associated with lesions in other organ systems with either metastasis to the globe or periocular areas (lymphoma, carcinoma, round cell tumor) or compression of the central nervous system (teratoma) (4,5,19,20). This emphasizes the need to perform a thorough diagnostic work-up, especially when the retrobulbar mass is challenging to access and sample. Computed tomography was useful in assessing the extent of lesions in the case described here, as well as in a similar case of retrobulbar round cell tumor reported in a macaroni penguin (15). Our case differs from that in the penguin in that the macaw's tumor was disseminated rather than localized, and diagnosis was achieved using *in vivo* hepatic cytology rather than at necropsy. Differential diagnoses for a retro-orbital mass, in addition to neoplasia, include retrobulbar granuloma (e.g., aspergillosis, mycobacteriosis, avian chlamydiosis, foreign body, and other bacterial or fungal granulomatous inflammation), hematoma, and trauma causing soft tissue swelling. Definitive diagnosis requires additional testing including cytology or histopathology; however, imaging can be used to direct sampling.

The presentation of birds with hepatic disease can be non-specific and highly variable, thus confirming a diagnosis often requires a multi-modal diagnostic approach (21,22). Hepatomegaly may be identified on palpation, or visualized directly through the transparent abdominal wall if the liver extends beyond the keel or suspected based on generalized coelomic distension (22,23). Alterations in biochemical parameters and/or radiographic changes suggestive of liver disease need to be followed by liver biopsy or fine-needle aspiration to definitively diagnose and characterize hepatic disease (22,23).

Humoral hypercalcemia of malignancy, more specifically, elevated ionized calcium levels in association with lymphoma, has been well-described in cats and dogs (24,25). This association has not been established in avian species; however, total hypercalcemia was reported in 2 Amazon parrots *(Amazona amazonica* and *Amazona aestiva)* diagnosed with malignant lymphoma (17). As ionized calcium was not measured, the presence of hypercalcemia of malignancy could not be confirmed. Total blood calcium levels were normal in the macaw described in the current report.

Coelioscopic examination and guided biopsy techniques under general anesthesia are well-described in the literature. This particular individual was deemed to be a poor surgical candidate due to elevated hepatic enzymes, previously identified arrhythmias, prolonged anesthetic recovery, and the presence of a marked hepatomegaly causing a coelomic mass-effect. As well, the owner was reluctant to pursue more invasive procedures. Consequently, fine-needle aspiration of the liver was performed. Ultrasound guidance was not necessary as the liver was readily visible under the skin just caudal to the sternum, and the CT had provided an excellent overview of hepatic size and shape. Aspiration cytology can vary in sample yield and diagnostic accuracy but in this case, with financial constraints and a poor surgical candidate, the technique allowed confirmation of diagnosis without the need to perform more invasive biopsy procedures. The cause of sudden death in this case was likely multifactorial, with hepatic neoplasia and ascites both contributing. The causes of ascites may include liver failure (clinical hypoproteinemia and elevated liver enzymes), portal hypertension, chronic passive congestion, or a secondary effect of neoplasia. Gastric hemorrhage may have resulted in the anemia identified on initial evaluation. The schwannoma noted in the pectoral musculature and the mild atherosclerosis are considered incidental findings. The heart histologically showed no evidence of disease, suggesting that the arrhythmia was due to a metabolic disturbance and or structural damage to the cardiac conduction system that was not evident histologically. As the bird died at home, examination of peripheral blood was not undertaken in order to determine whether the bird was leukemic terminally.

In the case described here, the cytologic and histologic appearances of the neoplastic cells were most consistent with a B-cell lymphoma with plasmacytoid differentiation. Immunohistochemistry is frequently used in domestic small mammal medicine to confirm and or identify the precise nature of lymphoid malignancies (26). Limitation exists when applying mammalian IHC regimens to the evaluation of tissue from pet avian species as no antibodies have been created specifically for immune-labelling of psittacine lymphocytes, and cross-reactivity may be poor. It is thus essential to include a positive control tissue, ideally from the same animal or at least from the same species, as well as positive and negative controls in a species for which the antibodies have been validated. While CD3 appears immunoreactive with a range of avian species (11,15,17,27), antibodies used routinely as B-cell markers on mammalian tissue; i.e., CD20 (rabbit polyclonal; Thermo Scientific, Burlington, Ontario), and CD79α (clone HM57, mouse monoclonal raised against the human antigen; Dako), do not react with avian lymphocytes in our experience. Hence, B-cell lymphoma has rarely been reported in the avian literature in comparison to cases confirmed as being of T-cell origin (18,27–29). One case report in an umbrella cockatoo *(Cacatua alba)* describes a cutaneous lymphoma of B-cell origin based on immunoreactivity with a rabbit monoclonal BLA.36 antibody (30). To the authors' knowledge staining of avian lymphocytes with this antibody has not been consistent or reliable, and thus was not attempted in this case. The use of MUM1 antibody for the identification of late phase B-lineage lymphocytes and plasma cells in avian species has not been reported to our knowledge, but in this case provided strong nuclear staining in neoplastic and control tissues. MUM1 staining was present in tissues from 3 species of psittacine birds, suggesting that this antibody may prove useful in differentiating lymphocytes in various members of the family Psittacidae.

Chemotherapy and/or palliative radiation has been reported as a treatment for neoplasia, especially for lymphoma, in birds (10,31). The umbrella cockatoo diagnosed with B-cell lymphoma was successfully treated with vincristine and chlorambucil (30). Due to the poor prognosis in the case reported here, as well as the reluctance of the owner to pursue intensive medical treatments, chemotherapy or radiation therapy was not attempted.

In conclusion, CT and fine-needle aspiration were used to investigate a retrobulbar mass and associated hepatic disease in a

yellow-collared macaw. This case illustrates how useful advanced imaging can be for defining retrobulbar lesions, which are difficult to assess using more traditional diagnostic methods, and shows that retrobulbar masses can be associated with disease in other organ systems; thus emphasizing the importance of a thorough and systemic diagnostic work-up regardless of presenting complaint. CVJ

References

1. Hawkins M, Barron H, Speer BLB, et al. Birds. In: Carpenter J, Marion C, eds. Exotic Animal Formulary. 4th ed. St. Louis, Missouri: Elsevier, 2013:184–438.
2. Beaufrère H, Nevarez JG, Holder K, Pariaut R, Tully TN, Wakamatsu N. Characterization and classification of psittacine atherosclerotic lesions by histopathology, digital image analysis, transmission and scanning electron microscopy. Avian Pathol 2011;40:531–544.
3. Gumpenberger M, Kolm G. Ultrasonographic and computed tomographic examinations of the avian eye: Physiologic appearance, pathologic findings, and comparative biometric measurement. Vet Radiol Ultrasound 2006;47:492–502.
4. Freeman KP, Hahn KA, Jones MP, Petersen MG, Toal RL. Unusual presentation of an Amazon parrot (Amazona species) with hepatocellular carcinoma. Avian Pathol 1999;28:203–206.
5. Rodriguez-Ramos Fernandez J, Dubielzig RR. Ocular and eyelid neoplasia in birds: 15 cases (1982–2011). Vet Ophthalmol 2014;18:1–6.
6. Platt SR. Evaluating and treating the nervous system. In: Harrison G, Lightfoot T, eds. Clinical Avian Medicine and Surgery. Palm Beach, Florida: Spix Publishing, 2005:493–518.
7. Gumpenberger M, Henninger W. The use of computed tomography in avian and reptile medicine. Semin Avian Exot Pet Med 2001; 10:174–180.
8. Morgan R. Magnetic resonance imaging of the normal eye and orbit of a screech owl *(Otus asio).* Vet Radiol Ultrasound 1994:362–367.
9. Coleman C. Lymphoid neoplasia in pet birds: A review. J Avian Med Surg 1995;9:3–7.
10. Reavill DR. Tumors of pet birds. Vet Clin North Am Exot Anim Pract 2004;7:537–560.
11. Schmidt V, Philipp HC, Thielebein J, Troll S, Hebel C, Aupperle H. Malignant lymphoma of T-cell origin in a Humboldt penguin *(Spheniscus humboldti)* and a pink-backed pelican *(Pelecanus rufescens).* J Avian Med Surg 2012;26:101–106.
12. Schnellbacher R, Wilson S. What is your diagnosis? Lymphoma. J Avian Med Surg 2010;24:241–244.
13. Ramos-Vara JA, Smith EJ, Watson GL. Lymphosarcoma with plasmacytoid differentiation in a scarlet macaw *(Ara macao).* Avian Dis 1997; 41:499–504.
14. Nevarez J, Doo-Youn C, Tully T. What is your diagnosis? J Avian Med Surg 2011;25:231–233.
15. Woodhouse S, Rose M, Desjardins D, Agnew D. Diagnosis of retrobulbar round cell neoplasia in a macaroni penguin *(Eudyptes chrysolophus)* through use of computed tomography. J Avian Med Surg 2014; 29:40–45.
16. Burgos-Rodríguez AG, Garner M, Ritzman TK, Orcutt CJ. Cutaneous lymphosarcoma in a double yellow-headed Amazon parrot *(Amazona ochrocephala oratrix).* J Avian Med Surg 2007;21:283–289.
17. de Wit M, Schoemaker NJ, Kik MJ, Westerhof I. Hypercalcemia in two Amazon parrots with malignant lymphoma. Avian Dis 2003;47: 223–228.
18. Souza MJ, Newman SJ, Greenacre CB, et al. Diffuse intestinal T-cell lymphosarcoma in a yellow-naped Amazon parrot *(Amazona Ochrocephala Auropalliata).* J Vet Diagn Investig 2008;20:656–660.
19. López RM, Múrcia DB. First description of malignant retrobulbar and intracranial teratoma in a lesser kestrel *(Falco naumanni).* Avian Pathol 2008;37:413–414.
20. Schelling S. Retrobulbar teratoma in a great blue heron *(Ardea herodias).* J Vet Diagn Investig 1994;6:514–516.
21. Jaensch S. Diagnosis of avian hepatic disease. Semin avian Exot Pet Med 2000;9:126–135.
22. Lumeij JT. Hepatology. In: Ritchie B, Harrison G, Harrison L, eds. Avian Medicine: Principles and Application. Lake Worth, Florida: Wingers Publishing, 1994:522–537.
23. Grunkemeyer VL. Advanced diagnostic approaches and current management of avian hepatic disorders. Vet Clin North Am Exot Anim Pract 2010;13:413–427.
24. Savary KCM, Price GS, Vaden SL. Hypercalcemia in cats: A retrospective study of 71 cases (1991–1997). J Vet Intern Med 2000:184–189.
25. Messinger JS, Windham WR, Ward CR. Ionized hypercalcemia in dogs: A retrospective study of 109 cases (1998–2003). J Vet Intern Med 2009;23:514–519.
26. Burkhard MJ, Bienzle D. Making Sense of lymphoma diagnostics in small animal patients. Clin Lab Med 2015;35:591–607.
27. Osofsky A, Hawkins MG, Foreman O, Kent MS, Vernau W, Lowenstine LJ. T-cell chronic lymphocytic leukemia in a double yellow-headed Amazon parrot *(Amazona ochrocephala oratrix).* J Avian Med Surg 2011;25:286–294.
28. Malka S, Crabbs T, Mitchell EB, et al. Disseminated lymphoma of presumptive T-cell origin in a great horned owl *(Bubo virginianus).* J Avian Med Surg 2008;22:226–233.
29. Kelly TR, Vennen KM, Duncan R, Sleeman JM. Lymphoproliferative disorder in a great horned owl *(Bubo virginianus).* J Avian Med Surg 2004;18:263–268.
30. Rivera S, McClearen JR, Reavill D. Treatment of nonepitheliotropic cutaneous B-cell lymphoma in an umbrella cockatoo *(Cacatua alba).* J Avian Med Surg 2009;23:294–302.
31. Graham J, Kent M, Théon A. Current therapies in exotic animal oncology. Vet Clin North Am Exot Med 2004;7:775–781.